NASA Technical Memorandum 80172

A Low Energy Electron Magnetometer

Jag J. Singh, George M. Wood, Jr.,
Grayson H. Rayborn, and Frederick A. White

DECEMBER 1979

NASA

NASA Technical Memorandum 80172

A Low Energy Electron Magnetometer

Jag J. Singh and George M. Wood, Jr.
Langley Research Center
Hampton, Virginia

Grayson H. Rayborn
University of Southern Mississippi
Hattiesburg, Mississippi

Frederick A. White
Rensselaer Polytechnic Institute
Troy, New York

National Aeronautics
and Space Administration

**Scientific and Technical
Information Branch**

1979

SUMMARY

Measurements of magnetic fields of the Earth and in space are expected to provide very useful information about geophysical characteristics, as well as interplanetary phenomena. Frequently, the magnetic fields involved are quite low (ranging from about 10^{-1} nT to 10^{5} nT), and measurement accuracies of the order of 1 percent or better are required for reliable interpretation of the magnetometer output. This paper analyzes the concept of a highly sensitive magnetometer based on the deflection of low energy electron beams in magnetic fields. Because of its extremely low mass and consequently high e/m ratio, a low energy electron is easily deflected in a magnetic field, thus providing a basis for very low field measurement. Calculations for a specific instrument design indicate that a low energy electron magnetometer (LEEM) can measure magnetic fields as low as 10^{-3} nT. The anticipated performance of LEEM is compared with that of the existing high-resolution magnetometers in selected applications. The fast response time of LEEM makes it especially attractive as a potential instrument for magnetic signature analysis in large engineering systems.

INTRODUCTION

Magnetic measurements are expected to provide useful information in a number of areas such as mineral prospecting surveys, planetary field measurements, and archaeological investigations, as well as laboratory studies. There are several types of magnetometers currently available, principal among which are: (1) Pivoted needle instruments which include the Swedish mine compass, the Hotchkiss superdip, and the Thalen-Tuberg magnetometers. The accuracy of these instruments seldom exceeds ±100 nT (1 nT = 1 gamma = 10^{-5} gauss), and they are not used much in current high-resolution applications. (2) The Schmidt and compensation-type variometers are precision magnetometers having accuracies better than ±5 nT, although their field accuracies are often in the range of ±(25 to 50) nT (ref. 1). (3) Fluxgate instruments can directly measure the vector components of the magnetic field. One property that makes fluxgate magnetometers suitable for ground as well as space use is their wide measurement range and low noise level. A sensitivity of 1 nT is routinely possible with airborne fluxgate meters, although sensitivities approaching 0.01 nT in the 0 to 10 Hz bandwidth and zero level stability of the order of ±0.1 nT have been reported for low field fluxgate meters designed for deep space missions (refs. 2 and 3). The NASA Goddard fluxgate magnetometers onboard Voyager 1 have been reported (ref. 4) to have a preliminary accuracy of ±0.2 nT ±0.1 percent of full scale. (4) Proton precession magnetometers measure precession of spin-alined protons around the test field after a strong magnetic field is removed from a sample of water. The spin-alined protons precess around the test field H at a frequency given by $g_p H$, where g_p is the proton gyromagnetic ratio. These magnetometers offer a sensitivity of 1 nT at a 1-sec sampling rate (refs. 4, 5, and 7). (5) Optically pumped magnetometers, such as helium and alkali vapor magnetometers, are among the most sensitive types of

magnetometers and can measure fields as low as 0.01 nT (refs. 5, 6, 8, and 9). (6) A superconducting quantum interference device (SQUID) is the most sensitive magnetometer today (refs. 5, 6, 10, and 11). A SQUID magnetometer is essentially a superconducting flux transformer tightly coupled to a SQUID and can routinely achieve resolutions of better than 10^{-5} nT/(Hz)$^{1/2}$. Frequently, SQUID magnetic field gradiometers are more practical than the absolute SQUID magnetometers. The gradiometers call for the use of a flux transformer with two pickup coils of equal area arranged to induce zero supercurrent in a uniform magnetic field and have reported sensitivities of less than 5×10^{-7} nT/cm/(Hz)$^{1/2}$.

To date, the fluxgate magnetometers have had the highest use in geomagnetic as well as interplanetary field mapping studies. These instruments have a routine sensitivity of ≈1 nT, although some designed for planetary and interplanetary field measurements have been reported to have much better sensitivities. (For example (ref. 12), the low field magnetometers on the Voyager 1 and 2 missions have an estimated absolute measurement accuracy of 0.09 nT, although changes in fields smaller than 0.09 nT can be detected since their observation is limited only by the sensor RMS noise (0.006 nT) and the quantization step size (0.004 nT for the most sensitive range).) Thus, it would appear reasonable to consider the development of an instrument that has a routine sensitivity of at least two orders of magnitude better (i.e., ≦0.01 nT). Among the existing instruments, there are two types that meet this sensitivity requirement, namely, the optically pumped magnetometers and the SQUID magnetometers. However, the SQUID magnetometer needs liquid helium for its operation. Hence, despite its extremely high stability and sensitivity, it seems destined to be used in the laboratory for special purposes only. The optical absorption magnetometers, which can measure the total field as well as the vertical gradients, have a routine sensitivity of <0.1 nT and are suitable for diverse laboratory and field (including space) applications. The rubidium magnetometer has commonly been used with low-altitude, Earth-orbiting satellites to obtain geomagnetic maps above the ionosphere. The Vector helium magnetometer has been flown on planetary missions to Mars, Venus, and Jupiter.

In this paper, a magnetometer concept based on the deflection of a low energy electron beam in the test field will be described. The sensitivity of a low energy electron magnetometer (LEEM) can compare quite favorably with that of the optical absorption magnetometers. Using state-of-the-art solid-state technology, LEEM response time can be reduced to microsecond range, thus making it especially appropriate for applications requiring fast magnetic transient analysis.

THEORETICAL BACKGROUND

Construction of electron-beam deflection magnetometers has been described by Cragg (ref. 13) and by Marton et al. (ref. 14). The instrument constructed by Cragg used a miniature cathode ray tube (CRT) in conjunction with a photomultiplier. A metal shutter obscured one-half of the CRT screen, dividing it along a diameter parallel to the deflecting plates. A feedback circuit automatically compensated the deflection of the electron beam by controlling the potential between the deflection plates of the CRT. A measurement of the

deflection potential thus constituted a determination of the magnetic field present in the device. Cragg (ref. 13) found that the limitation on the performance of his device was the instrumental drift amounting to 1 mV/min in the signal of 1.25×10^{-4} V/nT. He estimated, on the basis of a S/N ratio of 1, that the sensitivity of his device was about 10 nT, where the noise was the drift of the signal that occurred in a time of 1 min. Marton et al. (ref. 14), however, have demonstrated that the response of an electron-beam magnetometer can be pushed down to 2.9×10^{-10} A/nT and have actually constructed a device with a response of 3.15×10^{-10} A/nT. Assuming that a current of $\approx 3 \times 10^{-12}$ A could be detected easily, such a device would have a sensitivity of about 0.01 nT, equal to the sensitivity of the best alkali vapor devices.

Actually, good reason exists for believing that even a simple extrapolation of the Marton device, when used with a current-to-frequency converter (CFC), would provide greater sensitivity than the widely used alkali vapor magnetometers. The intrinsic sensitivity of the alkali vapor magnetometer is determined by the Larmor precession frequency of the alkali atom (3.498 Hz/nT for Cs and 4.667 Hz/nT for Rb (ref. 5)). Commercially available current-to-frequency converters produce 1 Hz/10^{-14} A. Thus, the sensitivity of an electron-beam device of Marton design using a current-to-frequency converter would be $\approx 3.15 \times 10^{4}$ Hz/nT (i.e., approximately two orders of magnitude higher than the Cesium vapor device for a minimum detectable current of 10^{-14} A).

ANALYSIS OF PARAMETERS LIMITING MAGNETOMETER SENSITIVITY

Problems associated with the design and construction of an electron-beam magnetometer can be appreciated by considering the device constructed by Marton et al. (ref. 14), which is shown in figure 1. Their instrument was 55 cm long, used a Steigerwald electron gun (ref. 15), and had an acceleration potential of 700 V, achieving an electron-beam current of $\approx 2 \times 10^{-8}$ A, with a filament temperature of $\approx$3000 K and a beam spot size of $\approx$100-μm radius. Detection was accomplished by dividing the beam image spot between two collector plates and measuring the difference in current between the two plates. The critical parameter in such a detection scheme is the current density distribution in the image spot at the plates. This is so because it is the current density that determines how much "difference" current is generated by a small change in the location of the center of the beam spot.

Figure 2 illustrates a simpler design suggested for an electron magnetometer. For direct comparison with the Marton instrument, it will be assumed that all essential parameters (electron energy, electron pathlength in test region, total electron-beam current in the image spot, and the image spot size) are the same in the two designs. The total current in the image spot, i_o, is given by

$$i_o = j(\pi R^2) \tag{1}$$

where j is current density and R is the radius of the image spot. A small shift in the position of the beam spot y results in shifting an area ΔA of the beam from one plate to another. The aerial beam shift ΔA is given approximately by

$$\Delta A \cong 2Ry \tag{2}$$

and aerial difference $2\Delta A$ between the two plates equals $4Ry$. If i_m is the minimum detectable current difference between the two plates, then the minimum detectable beam spot shift y_m is given by

$$y_m = \frac{i_m}{4Rj} \tag{3}$$

$$y_m = i_m \frac{\pi R}{4i_o} \qquad (\text{for } y_m << R) \tag{4}$$

For a pathlength L and acceleration potential V, this spot shift would be produced by a weak magnetic field B_o given by the following equation:

$$B_o = 2\left(\frac{2mV}{e}\right)^{1/2}\left(\frac{y_m}{L^2}\right) = 2\left(\frac{2mV}{e}\right)^{1/2}\left(\frac{i_m \pi R}{4i_o}\right)\left(\frac{1}{L^2}\right)$$

$$= \frac{1}{2}\left(\frac{2mV}{e}\right)^{1/2}\left(\frac{i_m}{i_o}\right)\left(\frac{\pi R}{L^2}\right) \tag{5}$$

where e and m are the electron charge and mass, respectively. Substituting the values of various parameters and assuming that $i_m = 1.0 \times 10^{-12}$ A gives

$$B_o = 2.32 \times 10^{-3} \text{ nT} \tag{6}$$

Thus, the sensitivity S of such a device would be

$$S = \frac{i_m}{B_o} = \frac{1 \times 10^{-12}}{2.32 \times 10^{-3}} \text{ A/nT}$$

$$= 4.31 \times 10^{-10} \text{ A/nT} \tag{7}$$

If the current from each collector plate was fed to a CFC device with a conversion factor of 1 Hz/10^{-14}, the system sensitivity would be $\cong 4.31 \times 10^4$ Hz/nT. Thus a measurement of magnetic field as low as 0.01 nT could be made with high accuracy in a 1-sec counting time. A measurement of 0.1 nT could be made with a moderate accuracy in a counting time of 10 msec.

An estimate of the dynamic range of the type of instrument described here could be made by determining the magnetic field B that would induce a 1-percent nonlinear response in the instrument. For instance, we note that

ΔA = Beam area change on a collector plate

$$= R^2\left[\frac{y}{R} \sin\left(\text{arc cos } \frac{y}{R}\right) + \text{arc sin } \frac{y}{R}\right] \tag{8}$$

The nonlinearity of the device is displayed in the following table:

Fraction of the range of instrument	Ratio of actual to measured magnetic field	Actual field,[a] nT
0.001	1.0000	0.059
.01	1.0000	.59
.05	.9996	2.95
.10	.9983	5.90
.20	.9933	11.80
.30	.9848	17.70
.40	.9727	23.60
.50	.9566	29.50
.60	.9363	35.40
.70	.9109	41.30
.80	.8796	47.20
.90	.8400	53.00
1.00	.7854	59.00

[a]The actual field has been determined for the specific instrument design parameters described earlier.

Thus the instrument as presently conceived is linear to ±1 percent over three decades (i.e., from under 10^{-2} nT to over 10^{+1} nT). Since the nonlinearity of the instrument is well understood, such nonlinearity could easily be removed in the course of data analysis and should not be detrimental to the successful operation of the instrument over a range of four decades (i.e., 5.9×10^{-3} to $5.9 \times 10^{+1}$ nT).

DISCUSSION OF LIMITATIONS ON SENSITIVITY

Figure 2 illustrated the schematic diagram of the instrument previously discussed. Its resolution is limited by the following factors:

1. Monochromaticity of the electron beam.

2. Uniformity of the beam spot on the collector plates. (This is directly related to the angular distribution of the electrons emitted from the source filament.)

Electron-Beam Monochromaticity

The deflection of the electron beam in the test magnetic field is dependent on the electron velocity. Because the hot filament source electrons (filament temperature ≈3000 K) can have an energy spread of ≅2 eV, the nominal energy of the electrons subjected to the magnetic field could range from 700.0 to 702.0 eV. This electron energy spread will produce a slight beam-spot distortion in magnetic field and may adversely affect the magnetometer sensitivity. However, an energy spread, $\Delta E/E = 3 \times 10^{-3}$, is negligible for a 1-percent accuracy instrument. In certain applications where $\Delta E/E$ must be $\gtrsim 10^{-4}$, it may be possible to obtain near-monoenergetic electrons using Rydberg atoms. (See appendix A for details.)

Beam-Spot Uniformity

Spatial uniformity of the beam is essential for optimal linear operation of LEEM. The spatial homogeneity of the beam can be assured by using low-divergence electron beams in an arrangement shown in figure 2. This arrangement should ensure symmetry, although not necessarily the uniformity, of the electron density distribution in the image spot. However, for a suitably designed hot filament emitting electrons randomly in all directions, this arrangement should provide both a symmetrical and a uniform intensity electron image spot on the collector plates.

As seen from equation (6), the sensitivity of LEEM is determined by the following parameters:

1. Electron energy

2. Electron pathlength in test field

3. Electron-beam intensity in the image spot

4. Image-spot size

It is possible to use lower electron energy without adversely affecting the resolution of LEEM if the initial energy straggle in thermionic emission could be eliminated. The thermionic energy straggle could be eliminated either by using an electrostatic analyzer or by using Rydberg atoms as discussed in appendix A. The electron pathlength of 55 cm cannot be increased much further without making the instrument impractical for certain applications (aerial survey or interplanetary field mapping). The electron image current could be increased by using field emission sources or by using a microchannel plate at the image location. Ordinarily, the image-spot size and the electron current go hand in hand. The reduction in image-spot size, effected by reducing the angle of divergence of incident electron beam, also results in reducing the electron-beam current. Perhaps the use of a focusing type of electron analyzer might simultaneously meet the requirements of higher electron image current and smaller image-spot size. Such an arrangement would also reduce the overall dimensions of the instrument and is described in appendix B.

For stationary applications, higher resolution could often be obtained if the instrument were used in a gradiometer arrangement. This would involve the use of two LEEM units, a convenient distance apart, operated simultaneously.

The electron-beam detection could also be more efficiently effected by using microchannel plates (ref. 16) instead of overlapping plate detectors considered earlier. The microchannel plates provide an additional gain of 10^4 (or 10^6 for compound plates), thereby making the S/N ratio considerably higher. The use of microchannel plates would appear to be particularly advantageous when the electron beam within an angle $2\alpha = 2 \times 10^{-4}$ rad is much less than 10^{-8} A. Detection of the change in the electron image-spot position on the channeltron plate can be effected with either a succeeding CFC device or a programed microprocessor incorporated in the microchannel plate circuit.

APPLICATIONS

Application in Mass Spectrometry

Measurements of mass spectrometer fringing fields are becoming more important as specialized mass spectrometers are being designed with inhomogeneous magnetic fields. Focal planes of greater than 1 m are currently being used for the simultaneous detection of ions. Further, the use of reverse-biased p-n junction detectors for detecting mass-spectrometer ion beams requires a more detailed knowledge of the external fringing field (ref. 17). Use of an electron-beam magnetometer to measure the fringing magnetic fields in a mass spectrometer would require the construction of a very small instrument, about 1 cm in length, since mapping of fringing fields involves determination of the spatial variation of a magnetic field over a distance on the order of 1 cm. Presumably the physical dimensions of the filament, aperture lens, and collector plates can be scaled down to permit the construction of a device as small as 1 cm.

The effect of such a shortened length on the sensitivity of the device can be determined by equation (6). The magnitude of the smallest detectable field change B_o is proportional to the square of the length L of the device. Thus, decreasing the length from 55 cm to 1.0 cm would decrease the sensitivity by a factor of $(55)^2$, or 3025. The new minimum detectable field would be $B_o = 7$ nT. Although performance of this instrument would be much less sensitive than the device previously discussed, it should be sufficient for field mapping and might prove useful in this regard. However, the sensitivity of such an instrument would not be substantially better than a good Hall effect gaussmeter.

Application in Archaeological Magnetic Surveying

Archaeological surveying requires both high sensitivity ($\approx$1 nT) and high spatial resolution, with readings sometimes needed as close together as every 10 cm (ref. 18). The alkali vapor magnetometer can apparently make magnetic field measurements with a sensitivity of 0.1 nT in a counting period of 10 msec, characteristics which are quite adequate for such work. An electron-

beam instrument would need to be built as small as the spatial variations which are to be observed (i.e., about 10 cm long). If an instrument were built to a length of 5.5 cm, with its other parameters as given before, it would have an expected sensitivity of approximately 4.31×10^2 Hz/nT ($\Leftarrow B_{min} = 0.23$ nT), which is not quite as good as an alkali vapor instrument. Thus, unless the electron-beam instrument could be built significantly cheaper than an alkali vapor instrument, the peculiar needs for spatial resolution in archaeological surveying would seem to favor the alkali vapor instrument over an electron-beam magnetometer.

Applications in Geophysical Prospecting

Aeromagnetic surveys have played an increasingly important role in geophysical prospecting since the early fifties. The magnetization of rocks, which arises from induction in Earth's field as well as their magnetic constituents, is usually surveyed with low-flying ($\leqq 300$ m) aircraft. Availability of higher resolution instruments should permit the survey craft to fly at a higher altitude (≈ 1 km), thereby permitting greater aerial coverage as well as reduced sensitivity to manmade interference. Usually, magnetometer sensitivities of the order of 0.1 nT have proved quite adequate for detecting magnetic anomalies associated with significant mineral deposits or outcrops. However, the recent development of optical absorption aeromagnetic gradiometers (refs. 5 and 6) with their higher sensitivities has improved the quality of aeromagnetic data considerably. Thus, LEEM, which is expected to be superior to the optical absorption magnetometer, should be even more useful in detecting finer magnetic anomalies associated with basement rocks buried beneath several hundred meters of nonmagnetic sediments or liquid hydrocarbons.

Applications in Mapping Interplanetary Fields

The strength of the interplanetary magnetic field is weak, having decreased to a value of about 5 nT at a distance of 1 astronomical unit, and is expected to continue to decrease with distance from the Sun, reaching a value of about 0.1 nT at the orbit of Uranus (ref. 19). Furthermore, the magnetic field of Venus is less than 10 nT and the field of our own Moon less than 1 nT at points on the surface (refs. 19 and 20) so that stringent requirements on sensitivity, accuracy, and dynamic range are imposed on any device measuring these fields. Any new instrument must at least meet, and possibly exceed, the requirements placed on the instruments used in the Pioneer and Voyager missions. For instance, the Pioneer 10 instrument was required to possess an accuracy of 0.025 nT and a sensitivity of 0.01 nT. That instrument was required to have a large dynamic range since the field of Jupiter was known to be several times 10^5 nT. In addition, minimal weight, ability to withstand launch vibrations, resistance to substantial nuclear radiation, and the maintenance of calibration under these conditions for a period of years were also the required characteristics of the instrument (ref. 19). Furthermore, the new instrument must be able to make vector measurements as required in planetary and interplanetary magnetic field measurement missions. It appears likely that an electron-beam deflection instrument incorporating three mutually orthogonal beams, derived from a common filament electron source, could be developed to meet all these

criteria. (It may even be possible to make a two-component field determination with a single beam instrument using a microchannel plate detector for measuring image-spot shift.) With further development and improvement in its beam-spot shift detection procedure, it is possible that the sensitivity requirement could be exceeded. This might prove to be an important consideration since some space missions may very well require greater sensitivity than can be provided by the existing magnetometers.

Detection of Phenomena Products by Fast Magnetic Transients

Some of the most intriguing as well as practical potential uses of an improved electron-beam magnetometer have yet to be made. In fact, a whole new field of "magnetic signature analysis" can be expected to complement other forms of spectroscopy. The basic challenge will be to develop a practical analytical device of high sensitivity, with a response time in the 10^{-7}-sec regime. Using charge-coupled devices in conjunction with microchannel plate amplifiers, exceedingly small electron-beam displacements can be correlated to fast transients.

In the general area of power transmission and distribution systems, there exists a need for precisely locating underground faults and monitoring electric utility substation circuitry. The detection of corona in high-voltage transmission lines and/or transformers presents another challenge. It has been suggested that the real-time "tracking" of lightning storms may be amenable to measurement by means of the remote sensing of lightning by multiple magnetometers. The final product testing of arc interrupters also makes use of magnetic signature analysis, for these devices are "packaged" so that a characterization of the arc discharge cannot be measured by optical or classical electrical measurements. Switches of all types could, in principle, be monitored remotely by means of this new form of nondestructive testing. Of course, some reference magnetic signatures would have to be established in order to indicate what is "normal," as opposed to those characterized by incipient failure.

There also exists a growing need for on-line, nonintrusive, real-time monitoring of motors and rotating machinery. Properly interfaced to a computer, electromagnetic signatures could complement other methods of checking electrical brushes and overall systems integrity. The fact that small magnetic transients can also accompany impact phenomena of some materials also suggests a possible application in loose-parts monitoring.

With an ultrafast response time, an electron-beam magnetometer can be utilized in the presence of slowly varying fields (i.e., 60 Hz). Instabilities in plasmas, the magnetic transients associated with arcs, ionizing gases, and the minute current variation in solid-state circuitry are all amenable to magnetic monitoring and testing. In research, it would also appear that magnetic signature analysis could ultimately be adapted for selected studies in electrochemistry and applied physics.

CONCLUSIONS

It has been shown that it should be possible to construct an electron-beam deflection magnetometer with a sensitivity of <0.01 nT. Use of a current-to-frequency converter might push the sensitivity of such a device to a much lower value or might permit the size and/or counting interval to be reduced below the proposed values of 55 cm and 1 sec. Indeed, the fact that such an instrument should produce a response of 4.31×10^4 Hz/nT (compared with 3.50 Hz/nT for a cesium vapor magnetometer) would seem to indicate that an instrument which would represent an enormous improvement in sensitivity and/or response time might be constructed. Such an instrument might have some liabilities for use in mass-spectrometer fringe field mapping or archaeological surveying, but it has definite possibilities for use in transient magnetic analysis in large system diagnostics, geophysical prospecting, and possibly interplanetary magnetic field studies.

Langley Research Center
National Aeronautics and Space Administration
Hampton, VA 23665
November 1, 1979

APPENDIX A

HIGH RYDBERG ATOMS AS MONOENERGETIC ELECTRON SOURCE

Recent advances in atomic physics have made it possible to excite atoms to very high quantum states. For these high Rydberg states, the Bohr model is legitimately valid. For example, the hydrogen-like states near the continuum may be defined by

$$E_n = -\frac{E_o}{n^2} \tag{A1}$$

where E_o is the 1S electron binding energy and n is the principal quantum number of the excited state. The radius of orbit n is

$$r_n = n^2 r_o \tag{A2}$$

where r_o is the 1S orbit radius. As is obvious from equation (A2), the atoms in the high Rydberg states can attain very large dimensions. Under these circumstances, the excited state electron is so far away from the rest of the atomic charge that the atom behaves like a weakly bound hydrogenic atom. When these high Rydberg state atoms collide with gaseous molecules, the following type of interaction takes place:

$$A^* + B \rightarrow A^+ + (B^- + \bar{e}) \tag{A3}$$

Because of the large radius of the Rydberg orbit, the interaction between the molecule B and the Rydberg electron takes place almost independently of the A^+ core. The A^+ core merely acts as a spectator in providing an almost free electron (the binding energy E_n in the Rydberg atom is ≤ 20 mV) (refs. 21 and 22).

It is the purpose of this appendix to indicate that equation (A3) can provide a means of producing nearly monochromatic low energy electron beams. If the Rydberg atoms can be produced in well-defined high n states, a collisional ionization experiment of the type illustrated in figure A1 can provide a beam of electrons of energy $E_{\bar{e}}$

$$E_{\bar{e}} = E_n + V_{acc} \cong V_{acc} \qquad \text{(because } E_n \leq 20 \text{ mV)} \tag{A4}$$

The following technique is suggested for producing Rydberg atoms in well-defined states (see fig. A2): a selected inert gas atomic beam is subjected to two pulsed dye lasers pumped synchronously by the same N_2 laser. One dye laser is used to saturate a suitable atomic state, which can then be excited to higher Rydberg states by the second tunable laser. These high Rydberg atoms are then allowed to pass through a He gas chamber, where electrons of energy $E_{thermal} - E_n$ (of order of a few millivolts) are produced. These near-zero energy electrons are then further accelerated in the manner shown in figure A1 to obtain low energy electron beams of desired energy.

APPENDIY A

An alternate scheme for producing near-monoenergetic electron beams would involve field ionization of the Rydberg atoms. A pulsed voltage, rising in a time of about 1 msec, is applied to a pair of conducting plates, 1 cm apart, to produce on the atoms a pulsed electric field of the order of 1000 V/cm. The field ionizes the Rydberg atoms and accelerates the electrons through a grid placed in the upper conducting plate. Figure A3 shows a schematic of this concept.

APPENDIX B

ELECTROSTATIC ANALYZERS AS MAGNETOMETERS

Electrostatic analyzers focus charged particles in an angle and disperse them according to their energy. They may thus be used as monochromators to define and select the energy of electrons that are thermionically emitted. Energy-selected electrons might be used in a magnetometer to avoid chromatic aberration in focusing, to decrease the spot size, and to increase the uniformity with which the electrons are deflected by the magnetic field. An electrostatic analyzer might also be used as an electron lens, replacing the lens used in the horizontal, rectilinear electron-beam magnetometer (ref. 14).

A number of electrostatic analyzer designs are available for use in a magnetometer: spherical, 127° cylindrical, cylindrical mirror, first-order parallel plate, and second-order parallel plate. The authors are aware of no literature on the effects of small magnetic fields on analyzers. For the purpose of presenting such a discussion, we choose to examine the simplest analyzer, the first-order parallel plate analyzer, although it may be that the second-order parallel plate analyzer, or the cylindrical mirror analyzer, would prove more useful in the actual design of a magnetometer because of the stronger, second-order focusing properties.

Consider an electron incident on the entrance slit of a parallel plate analyzer at an angle θ with the lower plate and at a speed of v_o. (See fig. B1.) If an electric field E, directed along negative Y-axis, exists between the plates to deflect the electron, then equations of motion are:

$$\ddot{x} = 0 \tag{B1}$$

$$\ddot{y} = -\frac{eE}{m} = a \tag{B2}$$

where a is the acceleration and e and m are the charge and mass of the electron, respectively, subject to the initial conditions

$$x(0) = y(0) = 0 \tag{B3}$$

and

$$\dot{x}(0) = v_o \cos \theta \tag{B4}$$

$$\dot{y}(0) = v_o \sin \theta \tag{B5}$$

Integration of the equations of motion leads to

$$x = (v_o \cos \theta)t \tag{B6}$$

APPENDIX B

$$y = (v_o \sin\theta)t - \frac{a}{2}t^2 \tag{B7}$$

so that the time required for the electron to return to $y = 0$ is

$$t^* = 2\frac{v_o}{a}\sin\theta \tag{B8}$$

at which time the electron has covered a range R in the x-direction, which is given by

$$R = \frac{2v_o^2 \sin\theta\cos\theta}{a} = \frac{v_o^2 \sin 2\theta}{a} \tag{B9}$$

It is easy to show that the range is a maximum for $\theta = \pi/4$, so that first-order focusing, $dR/d\theta = 0$, occurs for this angle. The maximum range R_o is given by

$$R_o = \frac{v_o^2}{a} = \frac{2K}{ma} \tag{B10}$$

where K is the kinetic energy of the nonrelativistic electron.

If a weak magnetic field B_o is also present and directed along the negative Z-axis, the equations of motion become

$$\ddot{x} = \frac{eB_o}{m}\dot{y} = \omega\dot{y} \tag{B11}$$

$$\ddot{y} = -a - \omega\dot{x} \tag{B12}$$

with $\omega = eB_o/m$, subject to the same initial conditions previously given. Integration of these equations leads to

$$x = \frac{1}{\omega}\left[\left(\frac{a}{\omega} + v_o\cos\theta\right)\sin\omega t + (v_o\sin\theta)(1 - \cos\omega t) - at\right] \tag{B13}$$

$$y = \frac{1}{\omega}\left[\left(\frac{a}{\omega} + v_o\cos\theta\right)\cos\omega t - 1 + (v_o\sin\theta)\sin\omega t\right] \tag{B14}$$

Since we are considering small magnetic fields, $\omega t << 1$ and $\omega v_o << a$. We may thus expand these last two equations, retaining first-order terms in ω, to obtain

APPENDIX B

$$x \cong (v_o \cos \theta)t + (v_o \sin \theta)\frac{\omega}{2} t^2 - \frac{\omega a}{6} t^3 \tag{B15}$$

$$y \cong (v_o \sin \theta)t - \frac{1}{2}(a + \omega v_o \cos \theta)t^2 \tag{B16}$$

One can see that the magnetic field changes the range of the electron in the analyzer by changing the time the electron remains in the analyzer and by altering the x component of velocity. The time required to return to $y = 0$ is

$$t^* = \frac{2v_o \sin \theta}{a + \omega v_o \cos \theta} \tag{B17}$$

Using the fact that $\theta = \pi/4$ for this analyzer, the range in the weak magnetic field correct to first order in $\omega v_o/a$ is then found to be

$$R = R_o\left(1 - \frac{\sqrt{2}}{3a} \omega v_o\right) \tag{B18}$$

and the change in the range ΔR caused by the magnetic field is

$$\Delta R = R_o - R = \frac{R_o \sqrt{2} \omega v_o}{3a}$$

Using equation (B10), this may be written as follows:

$$\Delta R = \frac{m}{\sqrt{2}} \omega v_o R_o^2 K^{-1} \tag{B19}$$

Finally,

$$\Delta R = \frac{1}{\sqrt{2}} eB_o m^{-1/2} K^{-1/2} R_o^2 \tag{B20}$$

This should be compared with the corresponding deflection Δy produced by a weak magnetic field B_o in a simple device discussed on page 4, where Δy is given by

$$\Delta y = \frac{eB_o}{2\sqrt{2}} m^{-1/2} K^{-1/2} L^2 \tag{B21}$$

Thus, for devices of similar length, $L = R_o$, the ratio of the deflections is

$$\frac{\Delta R}{\Delta y} = 2 \tag{B22}$$

Thus the deflection in the parallel plate analyzer would be twice as great as in a simple device of similar size. In addition, the use of an analyzer as a monochromator would decrease the spot size and would increase the uniformity with which the magnetic field deflects the electrons in the beam. These gains would, of course, be achieved at the cost of a loss in electron-beam intensity. Figure B1 shows a conceptual design of a low energy electron magnetometer using focused electron beams.

REFERENCES

1. Parasnis, D. S.: Principles of Applied Geophysics. John Wiley & Sons, Inc., c.1962.

2. Primdahl, F.: The Fluxgate Magnetometer. J. Phys. E: Sci. Instrum., vol. 12, no. 4, Apr. 1979, pp. 241-253.

3. Acuna, M. H.: Fluxgate Magnetometers for Outer Planets Exploration. IEEE Trans. Magn., vol. MAG-10, no. 3, Sept. 1974, pp. 519-523.

4. Ness, Norman F.; Acuna, Mario H.; Lepping, Ronald P.; Burlaga, Leonard F.; Behannon, Kenneth W.; and Neubauer, Fritz M.: Magnetic Field Studies at Jupiter by Voyager 1: Preliminary Results. Science, vol. 204, no. 4396, June 1, 1979, pp. 982-987.

5. Hood, Peter; and Ward, S. H.: Airborne Geophysical Methods. Advances in Geophysics, Volume 13, H. E. Landsberg and J. Van Mieghem, eds., Academic Press, 1969, pp. 1-112.

6. Hood, Peter J.: Geophysical Applications of High Resolution Magnetometers. Encyclopedia of Physics, Volume XLIX/3, Springer-Verlag, 1971, pp. 422-440

7. Baryshev, V. I.; Dekabrun, L. L.; Kil'Yanov, Yu. N.; Kuznetsov, A. A.; Poletayev, A. S.; and Chelyshev, V. I.: Stationary Precision Proton Magnetometer. Geomagn. & Aeron. (English Transl.), vol. 17, no. 6, June 1978, pp. 740-742.

8. Farr, W.; and Otten, E. W.: A Rb-Magnetometer for a Wide Range and High Sensitivity. Appl. Phys., vol. 3, no. 5, May 1974, pp. 367-378.

9. Stanley, J. M.; Ludbey, F. C.; and Green, R.: An Alkali Vapour Magnetometer Using Integrated Circuits. Space Sci. Instrum., vol. 1, no. 4, Nov. 1975, pp. 471-492.

10. Clarke, John: Josephson Junction Detectors. Science, vol. 184, no. 4143, June 21, 1974, pp. 1235-1242.

11. Steelhammer, T. J.; and Symko, O. G.: Calibration of SQUID Magnetometer for Dilute Alloy Studies. Rev. Sci. Instrum., vol. 50, no. 5, May 1979, pp. 532-534.

12. Behannon, K. W.; Acuna, M. H.; Burlaga, L. F.; Lepping, R. P.; Ness, N. F.; and Neubauer, F. M.: Magnetic Field Experiment for Voyagers 1 and 2. Space Sci. Rev., vol. 21, no. 3, Dec. 1977, pp. 235-257.

13. Cragg, B. G.: An Electronic Magnetometer. J. Sci. Instrum., vol. 32, no. 10, Oct. 1955, pp. 385-386.

14. Marton, L.; Leder, Lewis B.; Coleman, J. W.; and Schubert, D. C.: Electron Beam Magnetometer. J. Res. Natl. Bur. Stand., vol. 63C, no. 1, July-Sept. 1959, pp. 69-75.

15. Steigerwald, K. H.: Ein neuartiges Strahlerzeugungs-System für Elektronenmikroskope. Optik, Bd. 5, Heft 8/9, Apr. 1949, pp. 469-478.

16. Wiza, Joseph Ladislas: Microchannel Plate Detectors. Nucl. Instrum. & Methods, vol. 162, no. 1-3, June 1979, pp. 587-601.

17. White, F. A.: Mass Spectrometry in Science and Technology. John Wiley & Sons, Inc., c.1968.

18. Stanley, John M.; and Green, Ronald: Ultra-Rapid Magnetic Surveying in Archaeology. Geoexploration, vol. 14, no. 1, Jan. 1976, pp. 51-56.

19. Smith, Edward J.; Connor, Benjamin V.; and Foster, George T., Jr.: Measuring the Magnetic Fields of Jupiter and the Outer Solar System. IEEE Trans. Magn., vol. MAG-11, no. 4, July 1975, pp. 962-980.

20. Smith, Edward J.; and Sonett, Charles P.: Extraterrestrial Magnetic Fields: Achievements and Opportunities. IEEE Trans. Geosci. Electron., vol. GE-14, no. 3, July 1976, pp. 154-171.

21. Fabre, C.; Haroche, S.; and Goy, P.: Millimeter Spectroscopy in Sodium Rydberg States: Quantum-Defect, Fine-Structure, and Polarizability Measurements. Phys. Rev. A, third ser., vol. 18, no. 1, July 1978, pp. 229-237.

22. Percival, I. C.: Theory of Collisions With Highly Excited Atoms. Electronic and Atomic Collisions, G. Watel, ed., North-Holland Pub. Co., 1978, pp. 569-578.

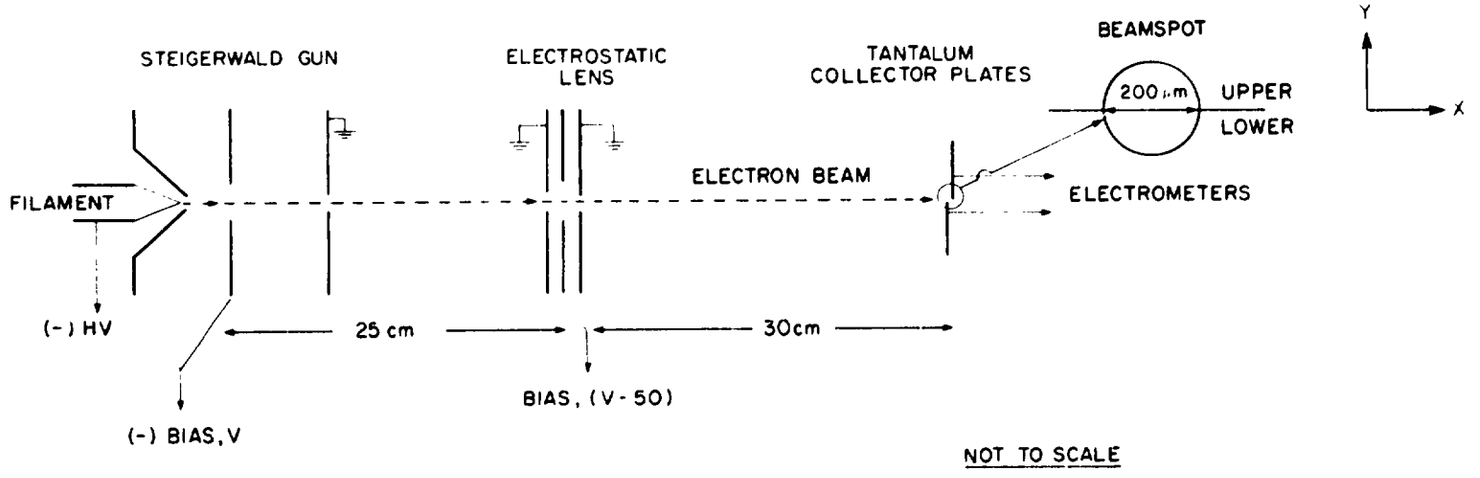

Figure 1.- Schematic diagram of electron-beam magnetometer designed by Marton et al (ref. 14).

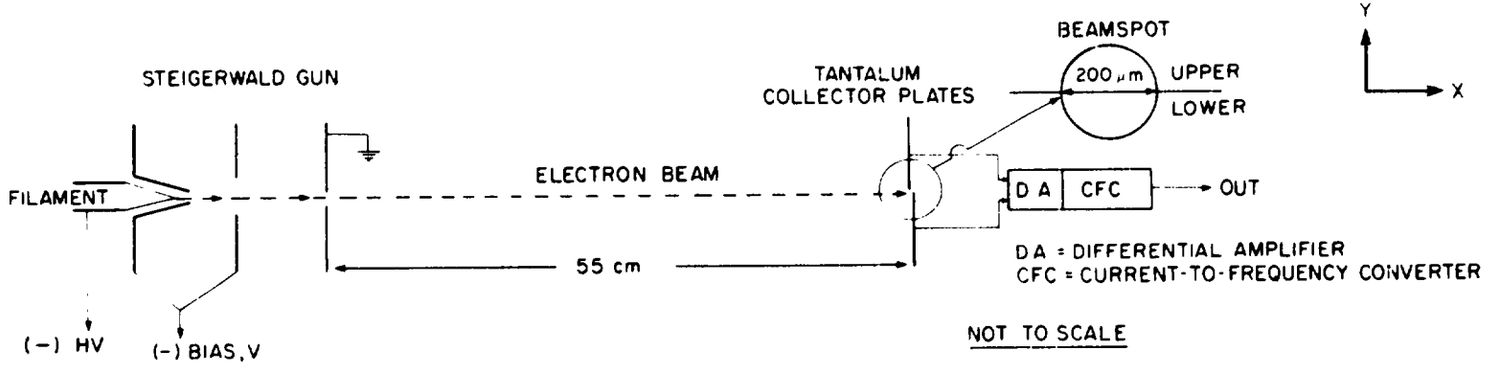

Figure 2.- Schematic diagram of low energy electron magnetometer discussed in present paper.

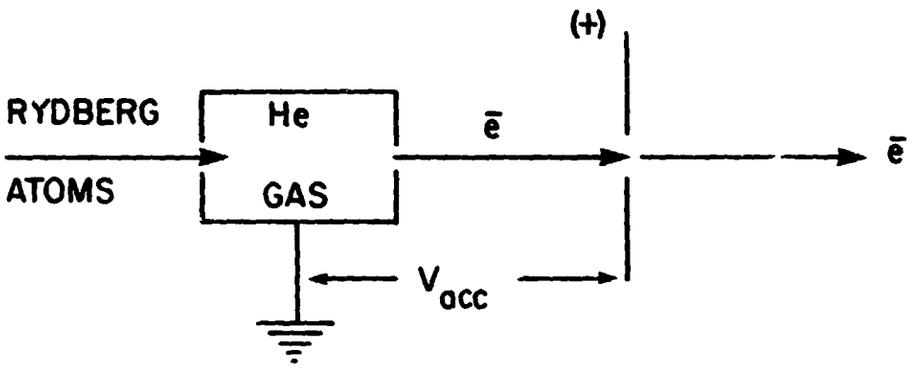

Figure A1.- Schematic diagram for producing monoenergetic electron beams.

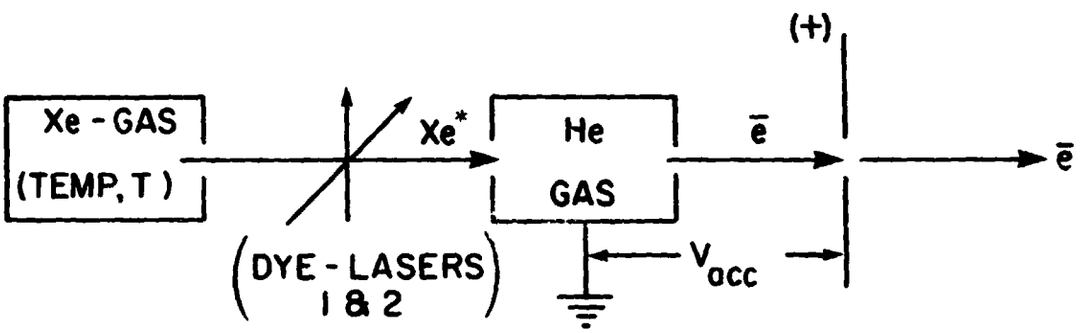

Figure A2.- Schematic diagram for producing low energy electron beams of well-defined energy.

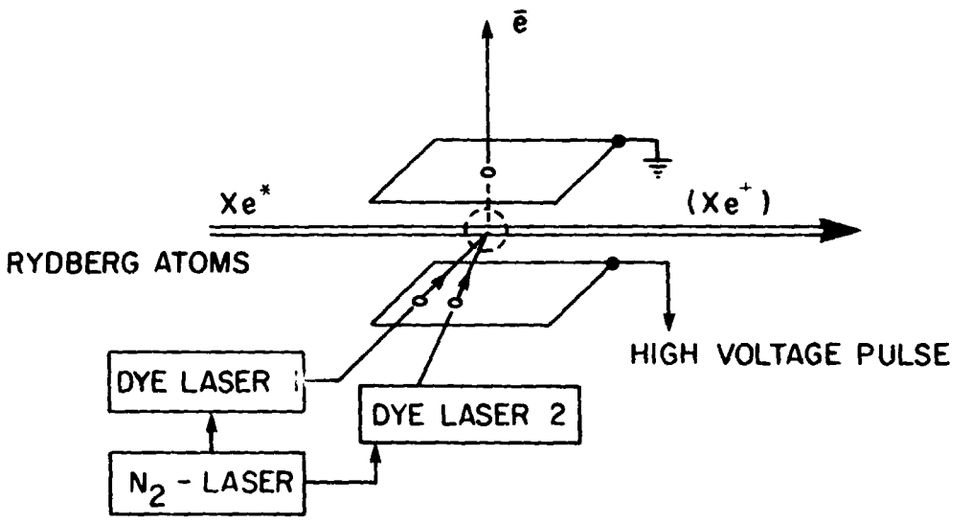

Figure A3.- Suggested scheme of experimental setup for field ionization of Rydberg atoms. Region of interaction between Rydberg atomic beam and lasers 1 and 2 becomes source of field emission electrons.

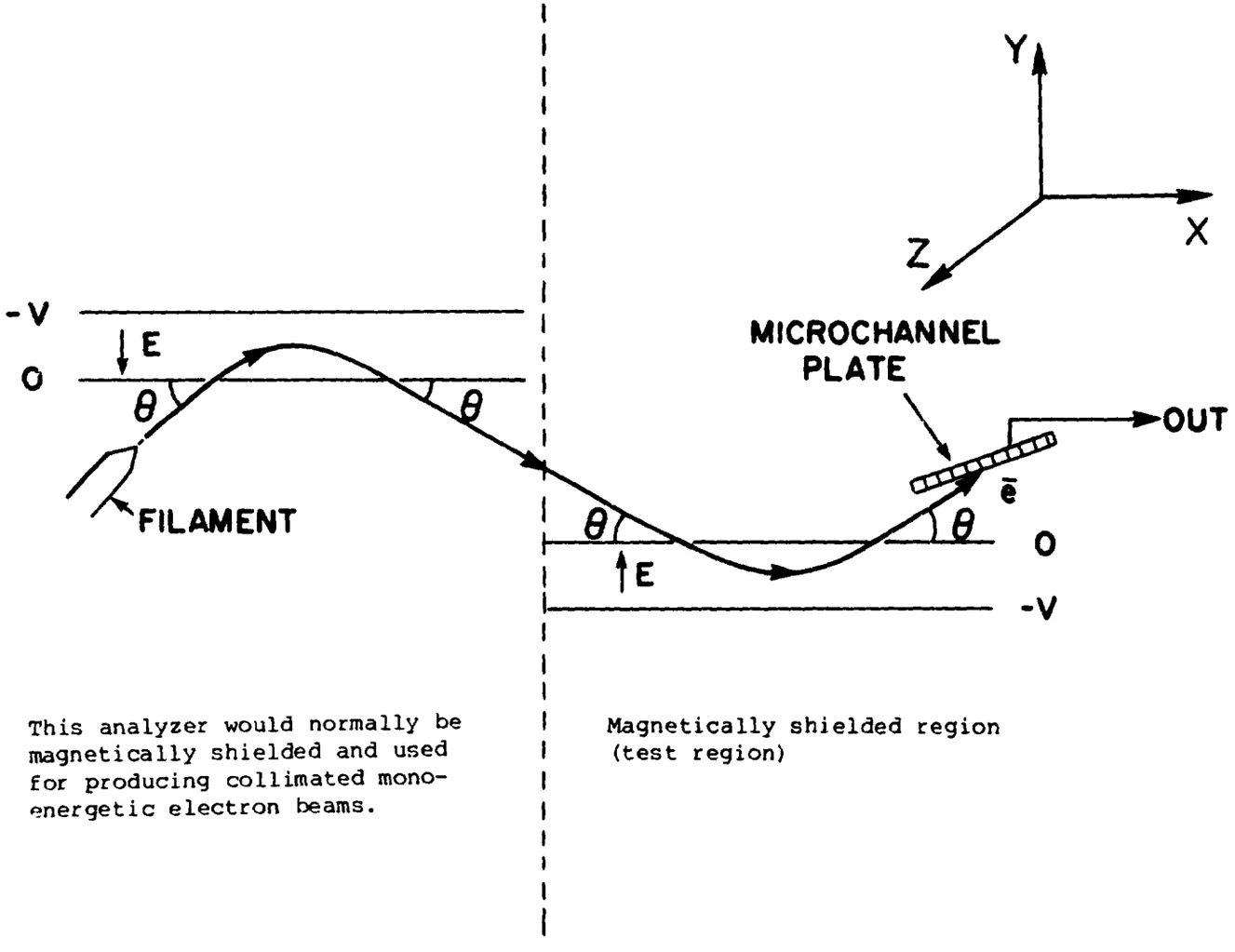

Figure B1.- Conceptual design of LEEM using focused electron beams.